Environ. Sci. Technol. **1998**, *32,* 1623−1628

Airborne Concentrations and Dry Deposition Fluxes of Particulate Species to Surrogate Surfaces Deployed in Southern Lake Michigan

MARIA J. ZUFALL,*,† CLIFF I. DAVIDSON,† PETER F. CAFFREY,‡ AND JOHN M. ONDOV‡

Department of Civil and Environmental Engineering, Carnegie Mellon University, Pittsburgh, Pennsylvania 15213, and Department of Chemistry and Biochemistry, University of Maryland, College Park, Maryland 20742

Dry deposition flux measurements to surrogate surfaces and airborne concentration measurements of Zn-containing, S-rich, and soil particles (analyzed by scanning electron microscopy) and Al, Ba, Br, Ca, Cl, Cu, K, Mg, Mn, Na, Ti, and V (analyzed by neutron activation analysis) were made over southwestern Lake Michigan in July 1994 and January 1995 to determine atmospheric inputs of pollutants to the lake. Samples collected in the summer show that despite relatively low airborne concentrations of particles with physical diameters >8 μm, these particles account for the majority of the dry deposition mass flux. However, this sharp contrast is not found during January when particles with physical diameters of 4−8 μm dominate both the airborne concentration and the flux. Dry deposition velocities (flux divided by airborne concentration) for particles are found to range from 0.0062 cm/s for 0.75-μm particles to 5.4 cm/s for 24-μm particles.

Introduction

Dry deposition of atmospheric contaminants to natural waters contributes to water quality degradation and may harm aquatic ecosystems. For example, eutrophication of lakes may be enhanced by excess inputs of nutrients (*1*), and toxic species deposition may harm aquatic life or make the plants and animals harmful to those higher on the food chain (*2*). Estimates show that dry deposition is responsible for a major fraction of total atmospheric deposition to the Great Lakes (*3*). Despite its importance, the number of measurements of pollutant dry deposition to bodies of water is limited, as are measurements of size-segregated deposition velocities needed for inferential estimates of deposition fluxes. A review of previously published studies is reported by Zufall and Davidson (*4*).

This is the second in a series of papers on dry deposition of particulate species to Lake Michigan. In the first paper, Caffrey et al. (*5*) report on elemental analyses of simultaneously collected airborne particle size distributions and deposition fluxes. The size distributions were measured using impactors, while the deposition fluxes were measured using aerodynamically designed surrogate surfaces. These data are used to estimate lower bounds for size-dependent deposition velocities to the lake for sampling periods in July 1994. In this second paper, we accomplish similar objectives through scanning electron microscopy and bulk chemical analyses of air filters and the surrogate surfaces. We also extend the data to include sampling periods in both July 1994 and January 1995. This research is part of the AEOLOS program (Air−Water Exchange over Lakes and Oceans) focusing on the transport of pollutants from sources to the Great Lakes and the Chesapeake Bay.

Experimental Section

Sampling. The data for this study were obtained aboard two cruises on Lake Michigan July 15−28, 1994, and January 15−19, 1995, when the RV *Lake Guardian*, a U.S. Environmental Protection Agency ship, was anchored at several stations in southwestern Lake Michigan. As described in the companion paper (*5*), the ship was always pointed into the wind during sampling to avoid contamination from activities onboard. During the July period, one set of samplers was placed on the bow, 5.2 m above the water surface, and an identical set was placed on the upper deck, 7.9 m above the water surface. In the January run, both sets of samplers were placed 5 m apart on the upper level of the ship due to limited sampling space on the bow. These locations were within 10 m of the sampling locations described by Caffrey et al. (*5*).

A filter system and identical Frisbee-shaped symmetric airfoils (*6, 7*) were used to measure airborne concentrations and dry deposition fluxes, respectively. The filter system included a 47 mm diameter polycarbonate filter, pore size 0.8 or 0.4 μm (Nuclepore 111107) in a stainless steel filter holder (Millipore XX5004710) and a Savillex Teflon filterpack with a 47 mm diameter, 1 μm Teflon Zefluor filter. The polycarbonate filter was analyzed by scanning electron microscopy (SEM), and the Teflon filter was analyzed by instrumental neutron activation analysis (INAA).

Zefluor Teflon filters coated with dimethylpolysiloxane (Dow Corning 200 Fluid) and upturned pieces of tape with liner (Ladd Research Company) were placed on the airfoils to measure dry deposition flux. The Teflon filters and the tape were analyzed by INAA and SEM, respectively.

Airborne concentration measurements were made daily, and dry deposition fluxes were measured over several days in order to obtain enough material for analysis. Both sets of measurements were stopped, and samples were covered during periods of rain or threat of rain. Table 1 lists the sampling period, exposure time, number of replicate samples, and the average wind speed for each SEM analyzed sample. Information on the INAA analyzed samples is given in Table 2.

Sample Analysis. An SEM with an energy-dispersive X-ray detector (EDX) was used to determine the size and elemental composition of individual particles collected in both airborne concentration and deposition samples. The EDX consists of a semiconducting crystal that absorbs X-ray photons to determine each particle's composition of elements with a molecular weight greater than Na (*8*). The SEM and EDX provide size and chemical data for particles between 0.2 and 300 μm in diameter (*9*).

The instrument used for this analysis was a computer-controlled SEM (CCSEM) developed by the R. J. Lee Group in Monroeville, PA. The CCSEM counted and analyzed at a magnification of 400× for particles with diameters between

* Corresponding author phone: (412)268-5811; fax: (412)268-7813; e-mail: mz25@andrew.cmu.edu.
† Carnegie Mellon University.
‡ University of Maryland.

S0013-936X(97)00645-7 CCC: $15.00
Published on Web 04/17/1998

TABLE 1. Sample Duration, Exposure Time, Number of Collocated Samples, and Average Wind Speed during Each Sample Period for SEM-Analyzed Samples[a]

samples	sample period	exposed time (h)	no. of samples	wind speed (m/s)
		Flux		
(1) 7/18−7/20	0100 July 18−0700 July 19	27.1	6	3.5
(2) 7/21−7/24	1300 July 21−0800 July 25	57.7	6	4.0
(3) 7/25−7/28	0800 July 25−1500 July 28	50.9	6	5.0
(4) 1/16−1/18	0900 Jan. 16−2000 Jan 18	43.7	6	5.3
		Concentration		
7/20 (1)	0100 July 18−0700 July 19	26.3	2	3.5
7/21 (2)	1300 July 21−0800 July 22	14.5	2	4.7
7/22 (2)	0800 July 22−2000 July 22	10.5	2	5.1
7/23 (2)	2000 July 22−0700 July 23	11.5	2	no data
7/24 (2)	1100 July 24−0800 July 25	20.0	2	3.3
7/25 (3)	0800 July 25−1900 July 25	10.2	2	4.8
7/26 (3)	0900 July 26−0600 July 27	20.0	2	3.4
7/27 (3)	0900 July 27−0700 July 28	18.5	2	6.3
7/28 (3)	0700 July 28−1500 July 28	6.0	2	5.9
1/17 (4)	0900 Jan. 16−2200 Jan 17	23.3	1	5.4
1/18 (4)	2200 Jan. 17−2000 Jan 18	21.2	2	4.7

[a] Wind speeds were measured on the ship. Time exposed is less than sample period due to cessation during rain episodes and boat movement. Concentration samples are listed with associated flux sample in parentheses.

TABLE 2. Average Airborne Concentrations and Dry Deposition Fluxes of Several Elements Analyzed by Neutron Activation[a]

element	concn (μg/m^3)	uncertainty (μg/m^3)	flux (μg m^{-2} h^{-1})	uncertainty (μg m^{-2} h^{-1})
Al	0.167	4.33E-03	7.88	0.651
Ba	7.98E-03	8.20E-04	0.195	0.0301
Br	1.19E-03	6.09E-05	9.11E-03	2.87E-04
Ca	0.481	0.0243	40.2	2.39
Cl	0.0601	0.0014	2.64	0.097
Cu	4.70E-3	5.13E-04	0.228[b]	0.0352
K	0.0652	0.0271	3.55	0.101
Mg	0.182	7.92E-03	10.8	0.648
Mn	9.03E-03	1.60E-04	1.39	0.0301
Na	0.0516	1.39E-03	1.46	0.0126
Ti	0.0150	1.13E-03	0.719	0.104
V	8.59E-04	2.14E-05	0.0376	1.35E-03

[a] Each concentration sample is the average of three 30-h samples taken during the same time periods as samples 7/23−7/28 in Table 1. Each flux is an average of values from samples taken during the same time period as flux samples 2 and 3 in Table 1. Uncertainties listed are 1 SD about the mean. Deposition velocities derived from these concentrations and fluxes are presented in Figure 6. [b] This value is for the 7/21−7/24 sample period only.

2 and 8 μm and at a magnification of 800× for particles between 0.25 and 2 μm until a total of 500 particles were found or 50 fields of view at each magnification were examined. Analyses were also conducted on 100 fields of view at a magnification of 200× for particles larger than 8 μm.

The data were then segregated by particle size and type. The particle size ranges based on the average dimension included (in μm): 0.25−0.5, 0.5−1, 1−2, 2−4, 4−8, 8−16, 16−32, 32−50, 50−100, and greater than 100 μm. The particle composition categories included organic compounds, anthropogenic metal-containing particles, S-rich, Cl-rich, and soil particles. The organics category included any particle with <500 X-ray counts obtained during the elemental composition analysis. This category represented particles with small amounts of elements with an atomic number greater than Na. These were most likely organic, but their exact composition was unknown. The anthropogenic metal-containing particles were defined as those which contained >5% of any one of the following metals: Hg, Pb, Cu, Zn, As, Sb, or Cd. Particles that are S-rich contained >30% S, and Cl-rich particles contained >30% Cl. Soil particles were those with <30% S and Cl and <5% of any of the metals in the list above and were generally rich in Al, Si, Fe, and/or Ca. A statistically significant number of particles was found for Zn-containing, S-rich, and soil particles, and the results of their analyses are presented here.

Particle number data were converted to mass data based on particle size and density. The particle volume (V) was calculated from projected area measurements according to $V = \pi/6D^2_{max}D_{min}$, where D_{max} and D_{min} are the maximum and minimum dimensions of the particle (*9*). This calculation assumes an oblate spheroid for irregularly shaped particles and reduces to the volume equation for a sphere when D_{min} equals D_{max}. The density of each particle was calculated as a weighted average based on elemental composition. The density of each element was based on the density of the most common oxides of that element. The mass per unit area of SEM field observed was computed for each particle composition category and size interval.

Due to the large number of particles collected on a single sample, only a small percentage of each sample was analyzed (~1%). Casuccio et al. (*9*) found the relative error between samples from the same filter analyzed by CCSEM ranged from 5% to 35%, with most of the error associated with particle composition categories that accounted for a small portion of the total mass. Duplicate analysis of the samples in this study found similar results. In addition, the agreement between collocated samples was reasonable, considering normal variability in ambient samples. The average relative error between collocated samples for a single species and size range was 55%. Again, greater error was associated with composition categories with smaller numbers of particles.

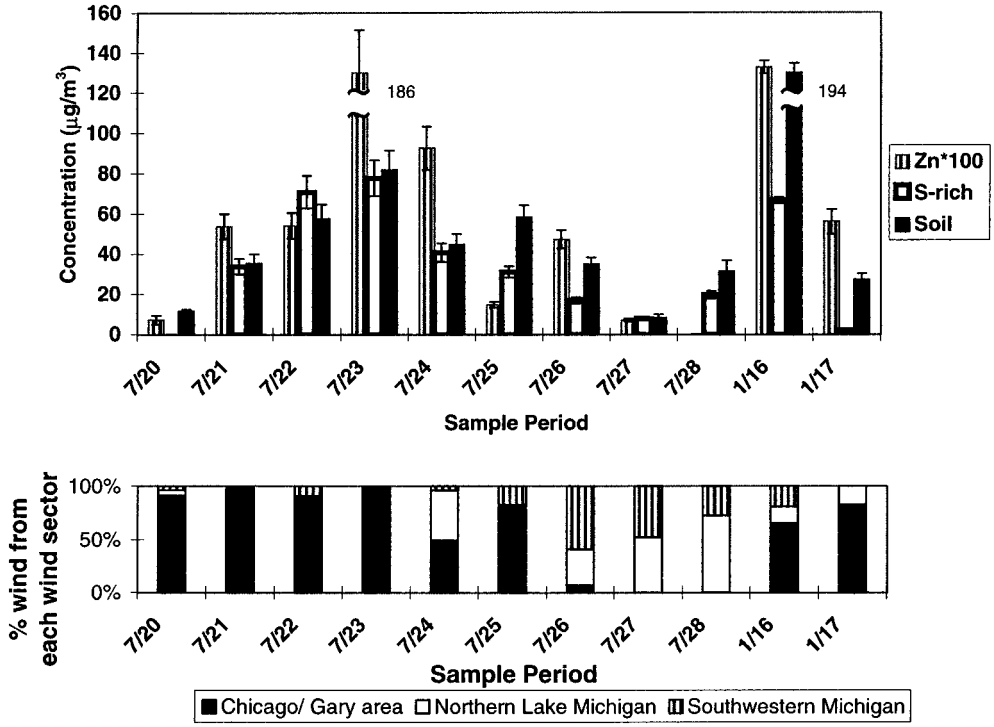

FIGURE 1. Airborne concentrations of Zn-containing, S-rich, and soil particles. Error bars represent the uncertainty in the measurement. Bottom graph shows percent of time that surface winds are out of each sector. Wind direction measurements were taken in Chicago.

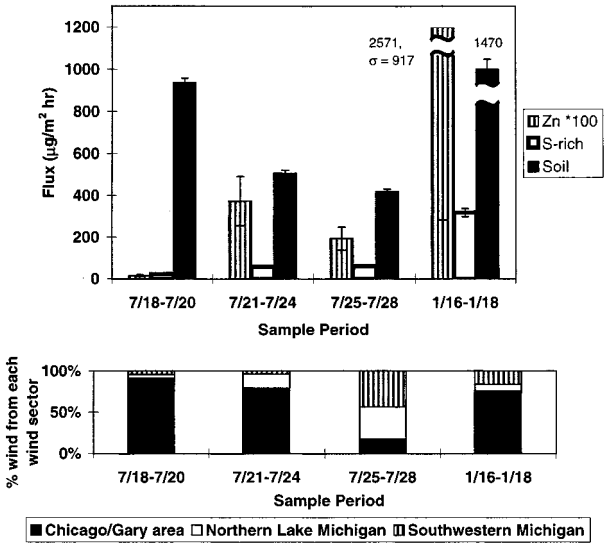

FIGURE 2. Dry deposition fluxes of Zn-containing, S-rich, and soil particles. Error bars represent the uncertainty in the measurement. Bottom graph shows percent of time that surface winds are out of each sector. Wind direction measurements were taken in Chicago.

A description of the methods used for INAA analysis is provided in the companion paper by Caffrey et al. (*5*).

Concentration, Flux, and Deposition Velocity Calculations. Airborne concentrations and dry deposition fluxes are shown in Table 2 and Figures 1 and 2. Analytical uncertainties were determined by propagating the uncertainties in the sample, blank, and, for airborne concentrations, flow rate measurements. For the SEM results, sample and blank uncertainties were calculated from counting statistics. For the INAA results, the sample and blank uncertainties were based on the counting statistics of the γ-ray peaks that were analyzed for each isotope. The combined uncertainty from two concurrent measurements was determined by taking one-half of the square root of the sum of the squares of the uncertainties from each measurement.

The deposition velocity was calculated from dry deposition flux divided by the corresponding time-averaged airborne concentrations:

$$V_d = F/C$$

Average deposition velocity ($\bar{V}_d$) curves for species analyzed by the SEM have been calculated from each sample period at each sample location. Values of $\sigma_{\bar{V}_d}$ represent one standard deviation about the mean of the individual deposition velocities. Deposition velocities of individual species were also calculated for INAA samples. The uncertainty associated with these values was determined from the uncertainty in the flux and airborne concentration measurements.

Results and Discussion

Airborne Concentrations. The airborne concentrations of Zn-containing particles, S-rich particles, and soil particles are shown in Figure 1, along with the percent of time that surface winds are out of each wind sector. For most samples, airborne concentrations when winds were primarily from the Chicago/Gary area (7/21−23, 1/16−17) were greater than those when winds were from the north and east (7/26−28). For example, concentrations were 10−25 times greater on July 23 as compared with July 27. The trend of increased soil particle concentration with winds from the southwest is most likely due to shorter transit times from shore. The enhancement of anthropogenic particles may be due to the proximity of the urban/industrial areas, although other factors (i.e., long-range transport) may be responsible.

Average airborne concentrations and dry deposition fluxes for elements determined by INAA are presented in Table 2. Airborne concentration values represent the average of three 30-h samples collected between 7/23 and 7/28, while the flux values represent an average of two samples collected during 7/21−24 and 7/25−28.

Dry Deposition Flux. Figure 2 shows the dry deposition fluxes of Zn-containing particles, S-rich particles, and soil

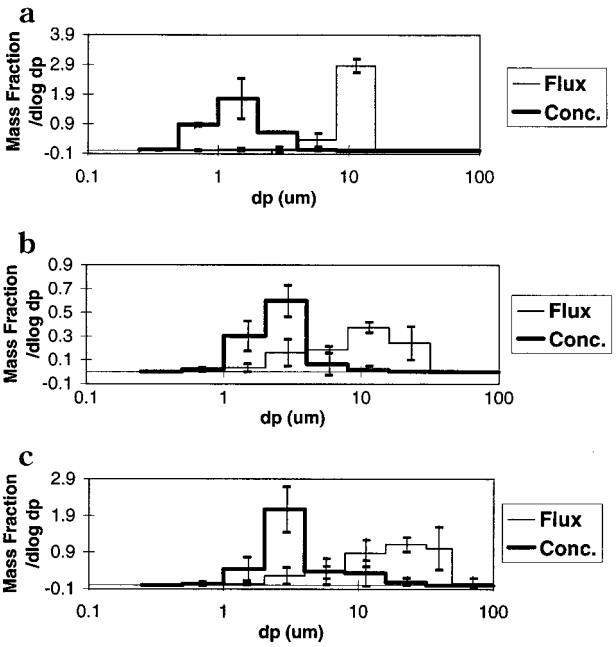

FIGURE 3. Mass fraction divided by the log of the physical particle size interval for concentration and dry deposition flux in each size range for July 1994 samples. Error bars represent one standard deviation and are not shown for categories with less than five total particles.

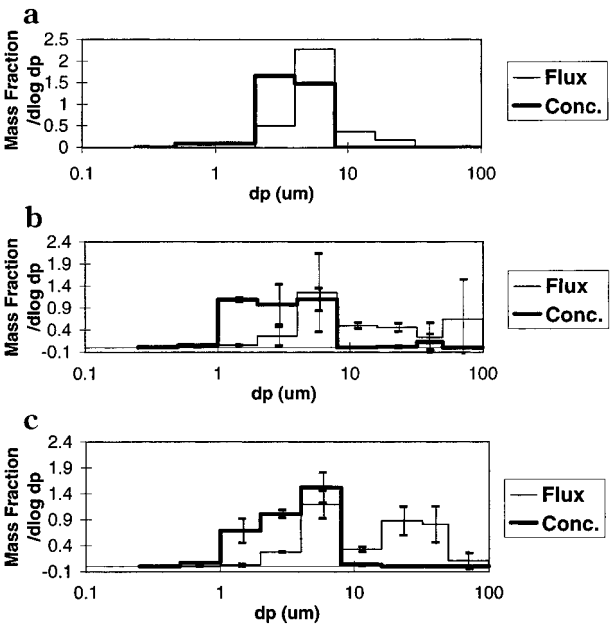

FIGURE 4. Mass fraction divided by the log of the physical particle size interval of concentration and dry deposition flux in each size range for January 1995 samples. Error bars represent one standard deviation and are not shown for categories with less than five total particles.

particles during the four sample periods along with the percent of time that surface winds are out of each wind sector. The flux measurements do not show a correlation to prevailing wind direction, as did most of the airborne concentration measurements. This is due to the greater averaging time of the flux samples and the many factors that influence dry deposition flux.

The measured fluxes to the surrogate surfaces are similar to other values reported in the literature. During the Lake Michigan Urban Air Toxics Study (LMUATS), dry deposition fluxes were measured to Mylar strips positioned on a smooth surface with a sharp leading edge (*10*) and estimated from a hybrid-receptor deposition model (*11*). Holsen et al. (*10*) measured total particulate mass flux over southwestern Lake Michigan in the summer to be approximately 1100 $\mu g\ m^{-2}\ h^{-1}$, which is comparable to the soil data presented here. Pirrone et al. (*11*) estimated the flux of Si and Ca particles less than 10 μm in aerodynamic diameter to be approximately 200 $\mu g\ m^{-2}\ h^{-1}$. The flux of soil-containing particles represents a significant fraction of the total mass flux and is comprised largely of Si and Ca. In addition, Zn mass flux determined from measurements was 1.6 $\mu g\ m^{-2}\ h^{-1}$ (*10*) and determined from modeling for particles with less than 10 μm aerodynamic diameter was 0.3 $\mu g\ m^{-2}\ h^{-1}$ (*11*) during LMUATS. These values are similar to the summer average of 2 $\mu g\ m^{-2}\ h^{-1}$ reported here. The fluxes estimated by the hybrid-receptor model are lower due to the exclusion of particles greater than 10 μm.

Mass Fraction in Each Size Range. Size distribution results from July 1994 show that the majority of dry deposition mass flux is from particles with a physical diameter greater than 8 μm, despite comprising less than 13% of the airborne concentration in the size ranges measured. The average mass fraction in each size category for concentration and flux for all of the summer samples is shown in Figure 3. This figure shows that the majority of the mass of airborne particles detected by the SEM are in the range of 1−4 μm in diameter. There are very few large particles (>8 μm) found in the air over the lake, due to the high-settling velocities of these largeparticles. The high-settling velocities also account for the large contribution of these particles to dry deposition flux. Although the deposition of small numbers of large particles can dominate the total mass flux of a species, the presence of these particles can be highly variable due to their low atmospheric concentrations. The important influence of large particles on dry deposition flux was also found by Holsen et al. (*10*).

The average mass fraction in each size category for concentration and flux samples from January is shown in Figure 4. These samples show an increase in particle mass in the 4−8 μm size range relative to the July samples for both airborne concentration and dry deposition flux measurements. The increase in concentration of these intermediate-sized particles is most likely due to wind speeds that were consistently higher and from the Chicago/Gary region during the January sample period. Although high wind speeds increase deposition velocities, they also decrease transit time from shore, thereby increasing the percentage of particles that reach the ship's location before depositing. In addition, high wind speeds increase the amount of particles derived from soil resuspension from land, which may contribute to the increase in airborne concentration of soil particles, especially in the 4−8 μm size range. Note that no snow cover was present during this sample period. The higher airborne concentrations of the 4−8 μm particles are responsible for the increased fluxes in January shown in Figure 2.

Dry Deposition Velocity. Figure 5 shows the experimentally determined dry deposition velocity curve (average for all particle categories and time periods, error bars represent one standard deviation about the mean), a dry deposition velocity curve as modeled by Williams (*12*), and deposition velocity results determined from a chemical mass balance method using measurements taken during the same sampling study (*5*). The experimental deposition velocities were calculated as the flux divided by the airborne concentration. The chemical mass balance model is described in Caffrey et al. (*5*). A density of 2 $g\ cm^{-2}$ is assumed to convert

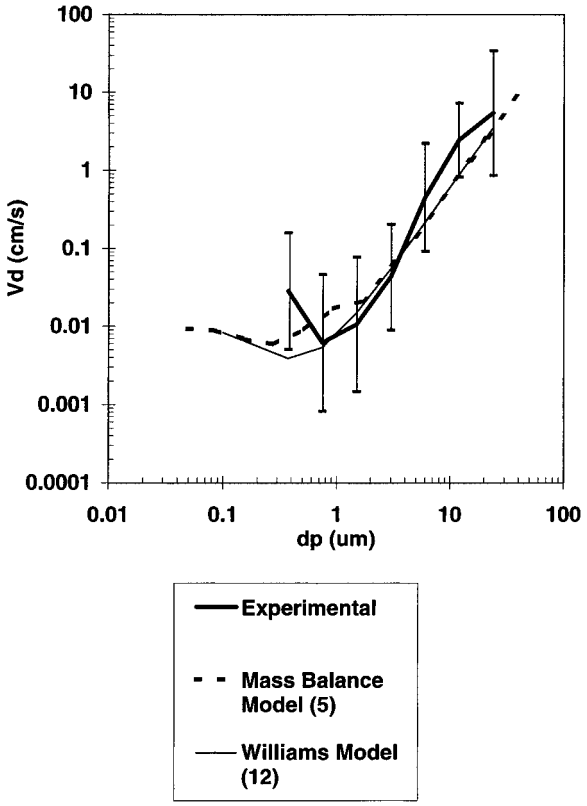

FIGURE 5. Dry deposition velocity vs physical particle diameter. Results are shown for the SEM data presented here with error bars representing variability among different particle types and sampling periods. In addition, a modified version of the Williams (*12*) model and results from a chemical mass balance model (*5*) are presented for comparison. Results shown from the Williams model are an average of runs using hourly meteorological data taken during all of the sampling periods.

impactor aerodynamic diameters to physical diameters. The Williams (*12*) model includes the effects of turbulent and Brownian diffusion, gravitational sedimentation, impaction, diffusiophoresis, hygroscopic growth, and breaking waves. However, the model results as shown here are modified so that the breaking wave and humidity terms are not included, since our measurements were made to a flat surface several meters above the water.

Measured deposition velocities are slightly higher than both the Williams (*12*) theoretical model and the Caffrey et al. (*5*) mass balance model for particles greater than 4 μm, while the measured values are slightly lower for particles between 0.5 and 4 μm. Overall, the agreement is quite good between both models and the experimental data. All curves follow the characteristic deposition velocity shape [see summary by Davidson and Wu (*13*)]. There is a minimum in the dry deposition velocity curve where the particle diameter is approximately 1 μm. This minimum occurs because small particles are deposited by Brownian diffusion, which is increasingly effective with decreasing particle size. Interception, inertial forces, and sedimentation transport larger particles with increased efficiency as particles become larger.

Figure 6 shows the deposition velocities determined for Al, Ba, Br, Ca, Cl, Cu, K, Mg, Mn, Na, Ti, and V for the 7/21–24 sample period. The deposition velocity for each element is plotted against the physical mass median aerodynamic diameter (mmad) for each element. The mmad was determined from size-segregated airborne concentration measurements taken with impactors during the same time period.

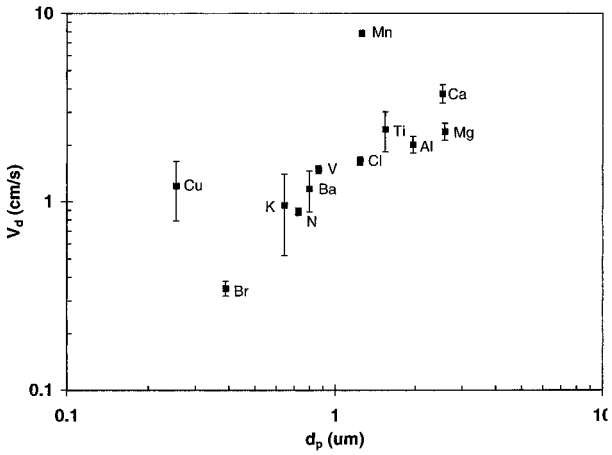

FIGURE 6. Dry deposition velocities for several trace elements plotted against physical particle mass median aerodynamic diameter (mmd). The mmd was determined from impactor measurements made during the same time period (*5*). Error bars represent the combined uncertainty in the concentration and flux measurements.

These impactor data can be found in Caffrey et al. (*5*). The mmad values for each element were calculated from the mass weighted average of the log of the midpoint d_p for each impactor stage and are in rough agreement with those reported elsewhere in the literature [see review paper of Milford and Davidson (*14*)]. Overall, the deposition velocity trend is similar to that exhibited in Figure 5.

Acknowledgments

The authors gratefully acknowledge Steve Eisenreich, Joel Baker, Tom Holsen, Jerry Keeler, and the crew of the RV *Lake Guardian* for providing assistance in the field. Logistical arrangements for sampling on the RV *Lake Guardian* were handled by Jackie Bode, U.S. Environmental Protection Agency. We would also like to thank Gary Casuccio and the staff at R. J. Lee for their assistance with the CCSEM. This work was funded by EPA Grant CR 82-2054-01-1 through a subcontract with the University of Michigan and by EPA Grant R-81-9897-01-0.

Literature Cited

(1) Henry, C. D.; Brezonik, P. L.; Edgerton, E. S. In *Atmospheric Pollutants in Natural Waters*; Eisenreich, S. J., Ed.; Ann Arbor Science Publishers: Ann Arbor, MI, 1981; pp 199–215.

(2) Thorton, J. D.; Eisenreich, S. J.; Munger, J. W.; Gorham, E. In *Atmospheric Pollutants in Natural Waters;* Eisenreich, S. J., Ed.; Ann Arbor Science Publishers: Ann Arbor, MI, 1981; pp 261–284.

(3) Gatz, D. *Water Air Soil Pollut.* **1975**, *5*, 239–251.

(4) Zufall, M. J.; Davidson, C. I. In *Atmospheric Deposition of Contaminants to the Great Lakes and Coastal Waters*; Baker, J., Ed.; SETAC Press: Pensacola, FL, 1997; pp 1–16.

(5) Caffrey, P. F.; Ondov, J. M.; Zufall, M. J.; Davidson, C. I. *Environ. Sci. Technol.* **1998**, *32*, 1615–1622.

(6) Wu, Y.-L.; Davidson, C. I.; Russell, A. G. *Aerosol. Sci. Technol.* **1992**, *17*, 231–244.

(7) Wu, Y.-L.; Davidson, C. I.; Russell, A. G. *Aerosol Sci. Technol.* **1992**, *17*, 245–262.

(8) Schwoeble, A. J.; Dalley, A. M.; Henderson, B. C.; Casuccio, G. S. *J. Met.* **1988**, *8*, 11–14.

(9) Casuccio, G. S.; Janocko, P. B.; Lee, R. J.; Kelly, J. F.; Dattner, S. L.; Mgebroff, J. S. *J. Air Pollut. Control Assoc.* **1983**, *33*, 937–943.

(10) Holsen, T. M.; Noll, K.; Fang, G.; Lee, W.; Lin, J.; Keeler, G. J. *Environ. Sci. Technol.* **1993**, *27*, 1327–1333.

(11) Pirrone, N.; Keeler, G. J.; Holsen, T. M. *Environ. Sci. Technol.* **1995**, *29*, 2112–2122.

(12) Williams, R. M. *Atmos. Environ.* **1982**, *16*, 1933–1938.

(13) Davidson, C. I.; Wu, Y.-L. In *Acidic precipitation*; Lindberg, S. E., Page, A. L., Norton, S. A., Eds.; Springer-Verlag: New York, 1990; pp 103−216.

(14) Milford, J. B.; Davidson, C. I. *J. Air Pollut. Control Asoc.* **1985**, *35*, 1249−1260.

Received for review July 23, 1997. Revised manuscript received February 10, 1998. Accepted February 19, 1998.

ES9706458